Journal of Computational and Applied Mathematics 429 (2023) 115234

Contents lists available at ScienceDirect

Journal of Computational and Applied Mathematics

journal homepage: www.elsevier.com/locate/cam

Mixed aleatory and epistemic uncertainty propagation using Dempster–Shafer theory

Yanyan He [a,*], M. Yousuff Hussaini [b]

[a] Department of Mathematics, and of Computer Science and Engineering, University of North Texas, Denton, TX, United States of America

[b] Department of Mathematics, Florida State University, Tallahassee, FL, United States of America

ARTICLE INFO

Article history:
Received 11 October 2022
Received in revised form 21 January 2023

Keywords:
Uncertainty propagation
Generalized polynomial chaos
Dempster–Shafer theory
Hausdorff distance
Epistemic uncertainty

ABSTRACT

In this paper, we deal with epistemic uncertainty in the framework of Dempster–Shafer theory, where basic belief assignments are used to characterize the uncertain parameters. To propagate the mixed epistemic and aleatory uncertainties, we introduce the relevant theoretical basics of DS theory, present the numerical approach based on DS theory combined with generalized polynomial chaos expansion, and conduct the error analysis for the numerical approach. Specifically, to analyze the convergence rate of the numerical solution represented with basic belief assignments, we define a measure based on the Hausdorff distance to quantify the difference between two basic belief assignments. The convergence of the numerical approximation is demonstrated with a few simple examples under different scenarios, and the presented numerical approach is applied to quantify the mixed types of uncertainty in quasi-one-dimensional flow.

1. Introduction

As computational power increases, numerical simulations have increasingly been used to study and predict the behavior of physical systems. However, due to the inherent variability of the systems, lack of understanding about physical characteristics, the assumptions embodied in the mathematical models, etc., uncertainty is inevitable in the modeling and simulation process. Therefore, to provide reliable information regarding the physical systems, quantifying the uncertainty in the simulations is critical.

Motivated by the need for uncertainty quantification (UQ) in simulations, there have been numerous attempts over the last few decade at developing UQ techniques. The predominant techniques characterize the uncertainty using random variables/processes in the framework of probability theory, such as the Monte Carlo method, generalized polynomial chaos (gPC) expansion and the stochastic collocation method [1–4], polynomial chaos-based kriging method [5]. However, in practice, the probability density functions (PDF) required by the probabilistic approaches may not always be available. In addition, there may exist uncertain parameters in the system, where the uncertainty is epistemic (referring to the uncertainty due to the lack of knowledge) rather than aleatory (referring to the uncertainty due to the random nature). In such situations, non-probabilistic approaches may provide a better representation of the epistemic uncertainty [6]. Notable non-probabilistic approaches are based on the alternative mathematical frameworks, such as interval analysis, fuzzy set theory [7,8], possibility theory [9,10], generalized *p*-boxes [11], and Dempster–Shafer (DS) theory [12,13]. Some of the research on epistemic uncertainty quantification using various approaches can be found in literature [14–21].

* Correspondence to: Departments of Math and of CSE, University of North Texas, 1155 Union Cir, Denton, TX 76203, United States of America.
E-mail addresses: yanyan.he@unt.edu (Y. He), yousuff@fsu.edu (M.Y. Hussaini).

https://doi.org/10.1016/j.cam.2023.115234
0377-0427/

Nomenclature

$(\mathcal{S}, \tilde{m})$	Finite support random set
$(\Omega, \mathcal{F}, \mathcal{P})$	Complete probability space
λ_i, Ψ_i	Eigenvalue, eigenfunction of C_{AA}
$\Phi_i(y)$	Generalized polynomial chaos
BBA	Basic belief assignment
CBF	Cumulative belief function
CDF	Cumulative distribution function
CPF	Cumulative plausibility function
$A(x)$	Cross-section area of nozzle
B_k	Focal element of $E_n(\xi)$
Bel, Pl	Belief and plausibility functions
$C_{AA}(x_1, x_2)$	Correlation of Gaussian process
$d(x_1, x_2)$	Euclidean distance
$d_H(A, B)$	Hausdorff distance between two sets
$D_H(m_f, m_g)$	Distance between two BBAs
D_k	High-dimensional focal element for ξ
$E(\xi)$	Expectation
$E_n(\xi)$	Approximation of expectation
m	m-function
P	Probability
p_1, p_2	Inlet, outlet pressure
$S(\xi)$	Standard deviation
$S_n(\xi)$	Approximation of standard deviation
u_i	gPC expansion coefficients
$u_n(\xi, y)$	gPC expansion over space Y
x_s	Shock position
Y	Stochastic space
Z	Non-probabilistic space or universal set

In the current work, we focus on the use of DS theory in uncertainty propagation (i.e., quantifying the uncertainty in outputs propagated from the uncertainty in inputs through the simulation model). Numerical techniques for epistemic uncertainty propagation based on DS theory have been explored and applied to various applications in the literature. For example, Oberkampf et al. have discussed the epistemic uncertainty propagation using DS theory and demonstrated the approach using an algebraic equation with two uncertain parameters [6]; Talavera et al. have applied DS theory to quantify the uncertainty in the paths that ships will navigate in the future, based on the information provided by the automatic identification system (AIS) on the paths followed by the ships in the past [22]; Tang et al. have quantified epistemic uncertainty in flutter analysis using DS theory to evaluate the structural stability and flutter risk of the system [23]; Abdallah et al. have utilized DS theory to model uncertainty in hydrographic inputs and analyzed their effect on climate change [24]; Bae et al. have proposed to use DS theory for quantifying the epistemic uncertainty that stems from lack of knowledge about a structural system, and further for the preliminary design of airframe structures in an intermediate complexity wing example [25]; Wang and Matthies [26] have used both DS theory and fuzzy set to represent the epistemic uncertainty and conduct reliability analysis, radial basis functions are constructed as a universal metamodel to improve the computational efficiency.

With the above-mentioned techniques, aleatory and epistemic uncertainties can be dealt with individually. However, mixed types of uncertainties normally exist in the underlying physical system and the simulation models. Therefore, it is necessary to explore the numerical UQ techniques for mixed aleatory and epistemic uncertainty propagation, which serves as the objective of our current work. Early attempts have been made to deal with the mixed uncertainties in the literature. For example, Roy and Oberkampf have discussed a comprehensive framework for estimating the predictive uncertainty of scientific computing applications based on the combination of probability theory and interval analysis, which results in a p-box to represent mixed types of uncertainties in the model output [19]. Baudrit et al. have presented a hybrid approach to jointly propagate and exploit probabilistic and possibilistic information in risk assessment, and proposed a new post processing method in the framework of DS theory [18]. DS theory has also been directly used for mixed types of uncertainty propagation. For example, Shah et al. have modeled both aleatory and epistemic uncertainty using DS theory and constructed a cheaper surrogate model for the response based on point-collocation non-intrusive polynomial chaos to reduce computational cost [27]. Tang et al. have combined DS theory with the gPC method to quantify the mixed types of uncertainty in synthetic problems, where DS theory is for epistemic uncertainty and gPC method deals with aleatory uncertainty [28]. Eldred et al. have implemented interval-valued probability, second-order probability and DS theory combined with probability theory for mixed types of uncertainty propagation where stochastic expansion methods are applied in stochastic space to reduce the computational cost [29]. These numerical approaches based on DS theory and probability theory with gPC method have worked effectively and efficiently for the synthetic examples and application problems. However, the above-mentioned research works provide only the minimum theoretical foundation of DS theory and no rigorous error analysis for the numerical approaches.

In this work, we introduce the relevant theoretical basics from DS theory, present the numerical approach based on DS theory combined with generalized polynomial chaos expansion, and conduct the error analysis for the approach. Specifically, we use definition of the extension principle for random sets directly in the framework of DS theory since the equivalence between basic belief assignments (defined in DS theory) and random sets has been discovered [30,31]. The extension principle uniquely defines the basic belief assignments (BBA) for model output mapped (through a function) from inputs characterized with BBAs [30]. Then we present the numerical approach for mixed types of uncertainty propagation in the system where gPC method is used for efficiently propagating aleatory uncertainty represented using PDFs and the extension principle is used for propagating epistemic uncertainty represented with BBAs. Since mixed types of uncertainties are involved, the BBAs corresponding to the statistics of model output will be obtained eventually. To implement the error analysis for the numerical approach, a distance to measure the difference between two BBAs is required. Various dissimilarity measures have been defined in the framework of DS theory and the thorough summary can be found in [32–34]. However, those measures are defined for BBAs with a set of finite number of elements as the universal set, therefore cannot be directly applied in the situation where the universal set is an interval. For the purpose of our current work, we define a distance measure based on the well-known Hausdorff distance to determine the difference between two BBAs.

This paper is organized as follows. We first provide a general problem setup in Section 2. Then we introduce relevant concepts from DS theory and define a new distance to measure the difference between two BBAs in Section 3. The numerical technique for mixed aleatory and epistemic uncertainty propagation and its theoretical error analysis are provided in detail in Section 4. In Section 5, we demonstrate the convergence of the numerical estimation using a few simple examples, and apply the numerical technique to quantify the mixed types of uncertainty in quasi-one-dimensional flow.

2. Problem setup

Let $x \in D \subset \mathcal{R}^{n_D}$ be the physical domain, and $t \in (0, T]$ $(T > 0)$ be the time domain. Let $Y \subset \mathcal{R}^{n_Y}$ be a bounded parameter domain for random inputs $y = \{y_1, y_2, \ldots, y_{n_Y}\}$ and $Z \subset \mathcal{R}^{n_Z}$ be another bounded parameter domain for other uncertain inputs $\xi = \{\xi_1, \ldots, \xi_{n_Z}\}$. n_D, n_Y and n_Z are the dimensions of the domain D, Y and Z, respectively. The random inputs characterize the aleatory uncertainty in the system while the other uncertain inputs represent the epistemic uncertainty in the system. Consider the following general partial differential equation

$$\begin{cases} u_t(x, t, y, \xi) = \mathcal{L}(u), & D \times (0, T] \times Y \times Z, \\ \mathcal{B}(u) = 0, & \partial D \times [0, T] \times Y \times Z, \\ u = u_0, & \bar{D} \times \{t = 0\} \times Y \times Z, \end{cases} \tag{1}$$

where u_t is the partial derivative $\partial u/\partial t$, $\mathcal{B}$ is the boundary condition operator, $u = u_0$ is the initial condition, and $\mathcal{L}$ is a differential operator. It is assumed that the problem is well-posed in $Y \times Z$, and the quantity of interest (u or a function of u) is continuous over domain Z.

We further assume that the probability density function is available for the random input y. However, no probability density function is assigned to the uncertain input ξ due to the lack of knowledge or data, and consequently the traditional probabilistic approaches are not applicable here. Instead, we assume that there exists sufficient information associated with ξ such that a BBA in the framework of DS theory can be constructed to model the uncertainty in ξ. The goal is to quantify the uncertainty in the model output $u(x, t, y, \xi)$, due to the mixed aleatory and epistemic uncertainty in the uncertain input variables y and ξ. Without losing the generality, we consider scalar model output (i.e., $u \in \mathcal{R}$).

3. Preliminaries

In this section, we will introduce the relevant concepts from DS Theory.

3.1. Basics of DS theory

Let $\xi \in Z$ be the quantity of interest, and the knowledge regarding ξ is incomplete and consequently the value of ξ is unknown. We consider the propositions in the form of "the true value of ξ is in A ($A \subset Z$)". The strength of evidence supporting the proposition A is represented by a belief function Bel in DS theory.

Definition 1. A belief function assigns a number in [0, 1] to an element $A \in 2^Z$ (Z is the universal set and 2^Z is its power set), satisfying:

$$Bel(\emptyset) = 0, \qquad Bel(Z) = 1,$$
$$Bel(\cup_{i=1}^{k} A_i) \geq \sum_{\emptyset \neq I \subseteq \{1,\ldots,k\}} (-1)^{|I|+1} Bel(\cap_{i \in I} A_i), \text{ for } k \geq 2, A_1, \ldots, A_k \in 2^Z.$$

Compare to probability density functions, belief functions do not have constraint of additivity. This relaxation makes them more flexible to represent epistemic uncertainty. Specifically, $Bel(A) + Bel(\bar{A}) \leq 1$, where $\bar{A}$ is the complement of A. When the summation does not reach one, the remaining part (i.e., $1 - Bel(A) - Bel(\bar{A})$) can support either A or $\bar{A}$ or even both (which cannot be specified due to lack of information), therefore, goes to universal set, representing part of the epistemic uncertainty. The dual measure of the belief function is called plausibility function ($Pl : 2^Z \to [0, 1]$), defined as $Pl(A) = 1 - Bel(\bar{A})$. It measures the maximum possible strength of evidence supporting a proposition A. Belief and plausibility functions can also be defined as

$$Bel(A) = \sum_{B \subseteq A} m(B), \qquad Pl(A) = \sum_{B \cap A \neq \emptyset} m(B), \tag{2}$$

where the basic belief assignment (BBA) $m : 2^Z \to [0, 1]$, also called m-function (hereafter we use BBA and m-function interchangeably), assigns a number (called mass or belief mass) in [0, 1] to an element $A \in 2^Z$, satisfying:

$$m(\emptyset) = 0, \qquad \sum_{A \subseteq Z} m(A) = 1. \tag{3}$$

Subset A is called a focal element if $m(A) \neq 0$. In this work, we assume the number of focal elements is finite.

The BBA can be interpreted using the concept of random sets (i.e., set-valued random variables) [30,31,35–37] as follows. Let Z be a non-empty set, a finite support random set on Z is a pair $(\mathcal{S}, \tilde{m})$ where $\mathcal{S}$ is a finite family of distinct non-empty subsets of Z and $\tilde{m}$ is a mapping $\mathcal{S} \to [0, 1]$ such that $\sum_{A \in \mathcal{S}} \tilde{m}(A) = 1$. The support of the random set $\mathcal{S}$ is equivalent to the collection of the focal elements for a belief function, and $\tilde{m}(A)$, which can be viewed as the probability of A containing the true value of variable ξ, is equivalent to the belief mass $m(A)$ for all $A \in \mathcal{S}$ [30]. The extension principle for random sets through a function is also defined in [30,35]. We state the definition in the language of DS theory as follows.

Definition 2. Let $u = f(\xi)$ be a mapping from the domain $Z \subset \mathcal{R}^{n_Z}$ to a domain U, and let m be the BBA associated with input variable ξ, where its focal elements are a finite number $\tilde{n}$ of subdomains $A_1, A_2, \ldots, A_{\tilde{n}}$ ($A_i \subset Z$), i.e., for any $A \subset Z$,

$$m_\xi(A) = \begin{cases} m_\xi(A_i), & \text{if } A = A_i, \qquad i = 1, \ldots \tilde{n}, \\ 0, & \text{otherwise,} \end{cases} \tag{4}$$

then the BBA of the output u (denoted as m_u) is defined as, for any $B \subset U$

$$m_u(B) = \begin{cases} \sum_{i \in S} m_\xi(A_i), S = \{i | f(A_i) = B\}, & \text{if } S \neq \emptyset, \\ 0, & \text{otherwise.} \end{cases} \tag{5}$$

Analogous to the cumulative distribution function in probability theory, cumulative belief function (CBF) and cumulative plausibility function (CPF) in DS theory are defined as follows.

Definition 3. Let Bel be a belief function in DS theory, then its cumulative belief function and cumulative plausibility function are [6,38]

$$CBF(z) = Bel(\xi \in (\infty, z]), \tag{6}$$
$$CPF(z) = Pl(\xi \in (\infty, z]). \tag{7}$$

Remark: Given the belief function, both CBF, CPF are obtained uniquely. However, the inverse does not hold, i.e., given a CBF and a CPF, we cannot get a unique belief function [38].

3.2. Distance between two BBAs

For the purpose of error analysis, we now introduce a distance to measure the difference between two BBAs or m-functions (the m-function obtained from numerical algorithms and the true m-function). Before that, let us first recall the commonly used distance — Hausdorff distance d_H between two non-empty sets A and B.

$$d_H(A, B) = \max \left\{ \sup_{x_1 \in A} \inf_{x_2 \in B} d(x_1, x_2), \sup_{x_2 \in B} \inf_{x_1 \in A} d(x_1, x_2) \right\}, \tag{8}$$

where $d(x_1, x_2)$ is a classical distance between elements x_1 and x_2.

For the purpose of our current work, we are interested in the distance between two BBAs defined over the real line. Therefore we rewrite the Hausdorff distance d_H for the special case with sets A, B being intervals and with the specification of $d(x_1, x_2)$ being Euclidean distance. Let $A = [a_1, a_2] \subset \mathcal{R}$ and $B = [b_1, b_2] \subset \mathcal{R}$ be two real intervals, the Hausdorff distance between A and B becomes

$$d_H(A, B) = \begin{cases} \max\{|a_1 - b_1|, |a_2 - b_2|\}, & \text{if all } |a_i|, |b_i| < \infty, i = 1, 2; \\ |a_1 - b_1|, & \text{if } |a_1|, |b_1| < \infty \text{ and } a_2, b_2 = \infty; \\ |a_2 - b_2|, & \text{if } a_1, b_1 = -\infty \text{ and } a_2, b_2 < \infty; \\ 0, & \text{if } a_1, b_1 = -\infty \text{ and } a_2, b_2 = \infty; \\ \infty, & \text{otherwise.} \end{cases} \tag{9}$$

Next we define the distance between two BBAs associated with the outputs from two functions of the same input variable.

Definition 4. Let $\xi \in Z$ be the input variable associated with a BBA (m-function) with finite number of focal elements $A_1, A_2, \ldots, A_{\tilde{n}}$ and the corresponding belief masses $m_\xi(A_1), m_\xi(A_2), \ldots m_\xi(A_{\tilde{n}})$. Consider two mappings f and g defined on Z, and the BBAs m_f and m_g for the corresponding outputs are defined by Definition 2. Denote $F_i = f(A_i)$ and $G_i = g(A_i)$. Then, the distance between the two BBAs m_f and m_g is defined as

$$D_H(m_f, m_g) = \sum_{i=1}^{\tilde{n}} m_\xi(A_i) d_H(F_i, G_i). \tag{10}$$

It satisfies the following properties:

- $D_H(m_f, m_g) \geq 0$ and $D_H(m_f, m_g) = 0 \Rightarrow m_f = m_g$.
- $D_H(m_f, m_g) = D_H(m_g, m_f)$.
- $D_H(m_f, m_g) \leq D_H(m_f, m_h) + D_H(m_h, m_g)$, where m_h is the BBA for the outputs of function $h(\xi)$.

Theorem 3.1. *Let $D_H(m_f, m_g)$ be the distance defined in Definition 4, where each of the focal elements $A_i \subset Z (i = 1, \ldots, \tilde{n})$ is a continuous domain and the two functions $f(\xi)$ and $g(\xi)$ are continuous over Z. If $|f(\xi) - g(\xi)| \leq \epsilon$ for any $\xi \in Z$, then $D_H(m_f, m_g) \leq \epsilon$.*

Proof. Since $|f(\xi) - g(\xi)| \leq \epsilon$ for any $\xi \in Z$, then $|f(\xi) - g(\xi)| \leq \epsilon$ for any $\xi \in A_i \subset Z$. In addition, $F_i = f(A_i) = [a_{1,i}, a_{2,i}] \subset R$ and $G_i = g(A_i) = [b_{1,i}, b_{2,i}] \subset R$ since f and g are continuous over the continuous domain A_i.

$$\begin{aligned} & D_H(m_f, m_g) \\ = & \sum_{i=1}^{\tilde{n}} m_\xi(A_i) d_H(F_i, G_i), \\ = & \sum_{i=1}^{\tilde{n}} m_\xi(A_i) * \begin{cases} \max\{|a_{1,i} - b_{1,i}|, |a_{2,i} - b_{2,i}|\}, & \text{if } |a_{j,i}|, |b_{j,i}| < \infty; \\ |a_{1,i} - b_{1,i}|, & \text{if } |a_{1,i}|, |b_{1,i}| < \infty \text{ and } a_{2,i}, b_{2,i} = \infty; \\ |a_{2,i} - b_{2,i}|, & \text{if } a_{1,i}, b_{1,i} = -\infty \text{ and } a_{2,i}, b_{2,i} < \infty; \\ 0, & \text{if } a_{1,i}, b_{1,i} = -\infty \text{ and } a_{2,i}, b_{2,i} = \infty; \\ \infty, & \text{otherwise} \end{cases} \\ & d_H(F_i, G_i) \neq \infty \text{ due to } |f(\xi) - g(\xi)| \leq \epsilon \text{ for any } \xi \in A_i. \end{aligned}$$

For the simplicity of writing, we omit the conditions for different scenarios.

$$D_H(m_f, m_g) = \sum_{i=1}^{\tilde{n}} m_\xi(A_i) * \begin{cases} \max\{|a_{1,i} - b_{1,i}|, |a_{2,i} - b_{2,i}|\}, \\ |a_{1,i} - b_{1,i}|, \\ |a_{2,i} - b_{2,i}|, \\ 0, \end{cases}$$

Since $|f(\xi) - g(\xi)| \leq \epsilon$ for all $\xi \in A_i$, we have $|a_{1,i} - b_{1,i}| \leq \epsilon$ and $|a_{2,i} - b_{2,i}| \leq \epsilon$ for the first case; $|a_{1,i} - b_{1,i}| \leq \epsilon$ for the second case; $|a_{2,i} - b_{2,i}| \leq \epsilon$ for the third case, therefore

$$D_H(m_f, m_g) \leq \sum_{i=1}^{\tilde{n}} m_\xi(A_i) * \begin{cases} \max\{\epsilon, \epsilon\}, \\ \epsilon, \\ \epsilon, \\ 0, \end{cases} \leq \epsilon \sum_{i=1}^{\tilde{n}} m_\xi(A_i) = \epsilon. \quad \square$$

4. Mixed aleatory and epistemic uncertainty propagation using generalized polynomial chaos and DS theory

In this section, we propose the numerical strategy for uncertainty propagation in the original problem Eq. (1). For the convenience of notation, we neglect the dependence of the solution on the variables x and t, and discuss the problem for any fixed $x \in D$ and $t \in (0, T]$. Then the output is denoted as $u(\xi, y)$. As mentioned in [15], this is a standard approach in most UQ literature.

As assumed in the problem setup, the epistemic uncertainty in the system is characterized by the uncertain non-probabilistic variable $\xi \in Z$ associated with a BBA, while the aleatory uncertainty is characterized by random variable $y \in Y$ associated with a probability density function. The mixed types of uncertainty are propagated through the system, and the goal is to mathematically represent the uncertainty in the output $u(\xi, y) : Z \times Y \to U$. Due to the availability of the probability density function (denoted as $\eta(y)$) for the random variable y, it is possible to evaluate the statistics of output u over the space Y, such as its expectation and standard deviation (denoted as S)

$$E(\xi) = E[u(\xi, y)|\xi] = \int_Y u(\xi, y)\eta(y)dy, \qquad \xi \in Z. \tag{11}$$

$$S(\xi) = \sqrt{E[u^2(\xi, y)|\xi] - E^2(\xi)} = \int_Y (u(\xi, y) - E(\xi))^2 \eta(y)dy. \tag{12}$$

Due to the mixed types of uncertainty, such statistics (e.g., $E(\xi)$, $S(\xi)$) are not deterministic. Instead, they are functions of the non-probabilistic variable ξ over the domain Z. Since a BBA is associated with the input variable ξ, the goal then becomes to obtain a BBA for the statistics of model output u efficiently.

4.1. Aleatory uncertainty propagation using GPC method

In this section, we adopt the gPC method to propagate the aleatory uncertainty in system, so that the statistics of the output solution u can be evaluated efficiently at a fixed ξ. For simplicity, we denote the output $u(\xi, y)$ at a fixed ξ as $u(y)$.

First we define a complete probability space $(\Omega, \mathcal{F}, \mathcal{P})$, where Ω is the sample space including all possible outcomes, $\mathcal{F} \subset 2^{\Omega}$ is the σ-algebra with all measurable events belonging to Ω, and $\mathcal{P} : \mathcal{F} \to [0, 1]$ is the probability measure. Assume that the uncertainty in a system is represented by a set of uncorrelated random variables $y = \{y_1(\omega), y_2(\omega), \dots, y_{n_Y}(\omega)\} : \Omega \to Y \subseteq \mathcal{R}^{n_Y}$. Then any second-order random variables $u(\omega) \in \mathbf{L}_2(\Omega, \mathcal{P})$ can be approximated by a gPC expansion as follows [2,39–41]:

$$u_n(y(\omega)) = \sum_{i=0}^{N-1} u_i \Phi_i(y(\omega)), \tag{13}$$

where n is the highest polynomial order, $N = (n_Y + n)!/(n_Y!n!)$ is the number of terms, and u_is are the gPC coefficients to be determined in the algorithm. The functions Φ_i were originally proposed as Wiener–Hermite polynomial chaos (under assumption of y associated with Gaussian distribution) by Wiener [1] and later extended to the generalized polynomial chaos via the Askey scheme [2]. The choice of the type of the polynomial chaos depends on the distribution of the random inputs. By matching the probability density function (PDF) of random variables to the weighting function of orthogonal polynomials, the gPC expansion with this specific type of polynomial basis is capable of converging rapidly to a smooth function. In the current work, we adopt the corresponding polynomials from Askey scheme for random variables with different distributions.

Using the orthogonality of the polynomial basis, one can calculate the gPC coefficients by projecting u on each basis with the inner product

$$u_i = \frac{\langle u, \Phi_i \rangle}{\langle \Phi_i, \Phi_i \rangle} = \frac{1}{E[\Phi_i^2]} \int_Y u(y)\Phi_i(y)\eta(y)dy, \tag{14}$$

where $\eta(y)$ is the PDF of the variable y, and the integration can be approximated using a quadrature rule as

$$u_i \approx \hat{u}_i = \frac{1}{E[\Phi_i^2]} \sum_{j=1}^{M} u(y^{(j)})\Phi_i(y^{(j)})\alpha^{(j)}, \qquad i = 0, 1, \dots, N-1, \tag{15}$$

where $\{y^{(j)}, \alpha^{(j)}\}_{j=1}^{M}$ is a set of quadrature points and the corresponding weights. Sparse grid quadrature points can be considered for high-dimensional stochastic space since the number of quadrature points increases exponentially as the dimension increases [42].

For the output $u(\xi, y)$ with variable ξ, the truncated gPC expansion (as in Eq. (13)) is updated as

$$u_n(\xi, y) = \sum_{i=0}^{N-1} u_i(\xi)\Phi_i(y), \tag{16}$$

where the gPC coefficients depends on the variable ξ. The gPC expansion u_n approximate u accurately for each $\xi \in Z$ and the convergence of u_n (for any ξ) can be expressed as

$$\epsilon_n(\xi) = \|u_n - u\|_{L^p_\eta(Y)} \to 0, \qquad p \geq 1, \text{ as } n \to \infty, \tag{17}$$

More details on gPC can be found in [2,41].

Since u_n is an approximation to u, then the statistics of the output such as $E(\xi)$ (and $S(\xi)$) can also approximated by E_n (and $S_n(\xi)$) as

$$E_n(\xi) = E[u_n(\xi, y)|\xi] = \int_Y u_n(\xi, y)\eta(y)dy, \qquad \xi \in Z. \tag{18}$$

$$S_n(\xi) = \sqrt{E[u_n^2(\xi, y)|\xi] - E_n^2(\xi)} = \int_Y (u_n(\xi, y) - E_n(\xi))^2 \eta(y)dy. \tag{19}$$

Similarly, the quantities E_n and S_n are functions of variable ξ. With gPC expansions u_n over the stochastic space Y, the expectation and standard deviation can be obtained directly from the gPC coefficient u_is as

$$E_n(\xi) = u_0(\xi)E[\Phi_0^2(y)]; \qquad S_n(\xi) = \sqrt{\sum_{i=1}^{N-1} u_i^2(\xi)E[\Phi_i^2(y)]}. \tag{20}$$

4.2. Epistemic uncertainty propagation using DS theory

Consider the numerical approximation expectation E_n (function of $\xi = \{\xi_1, \ldots, \xi_{n_Z}\}$) as an example (the standard deviation $S_n(\xi)$ can be considered with the exact same procedure by replacing $E_n(\xi)$ with $S_n(\xi)$). Uncertainty propagation using DS theory is to find the BBA (m-function) for the output E_n given the BBAs for each ξ_i.

Suppose the universal set $Z_i = [a_i, b_i]$ ($1 \leq i \leq n_Z$) includes all the possible values of ξ_i. And the focal elements are a finite number of subintervals $D_{ij} = [a_{ij}, b_{ij}]$, where $1 \leq j \leq \tilde{n}_i$ and $\tilde{n}_i < \infty$ is the number of focal elements of the BBA m_i.

The n_Z-dimensional belief structure of the BBA can be constructed by taking the Cartesian product over all the directions of ξ. Specifically, the universal set is $Z = Z_1 \times Z_2 \times \cdots \times Z_{n_Z}$. The focal elements are $D_k = D_{1k_1} \times D_{2k_2} \times \cdots \times D_{n_Z k_{n_Z}}$ for $1 \leq k \leq \prod_{i=1}^{n_Z} \tilde{n}_i$, where D_k is a n_Z-dimensional hypercube, and D_{ik_i} is a focal element of the ith BBA m_i. The mass of each focal element is $m_\xi(D_k) = \Pi_{i=1}^{n_Z} m_i(D_{ik_i})$. Note that the focal elements of the BBA for n_Z-dimensional variable ξ may not be hypercubes if the BBA for ξ is directly prescribed (instead of the BBAs for each ξ_i).

The uncertainty in ξ, represented by the n_Z-dimensional belief structure, is propagated through the function $E_n = E_n(\xi)$ and accumulated in the uncertainty of the output E_n. The BBA of the output E_n based on Definition 2 can be used to represent the uncertainty in E_n. For the purpose of numerical computation, we construct the BBA by first solving a pair of optimization problems in each hypercube D_k.

$$B_{k,1} = \min_{\xi \in D_k} E_n(\xi), \tag{21}$$

$$B_{k,2} = \max_{\xi \in D_k} E_n(\xi). \tag{22}$$

Under the assumption that the output u is continuous in Z, the interval $B_k = [B_{k,1}, B_{k,2}]$ becomes one focal element of the BBA for $E_n(\xi)$, and the belief mass is $m_\xi(D_k)$. Obviously, the BBA of the output $E_n(\xi)$ should have the same number of focal elements as the BBA of ξ unless there are more than one hypercubes corresponding to the same focal element for $E_n(\xi)$.

The error in the obtained BBA for the numerical approximation $E_n(\xi)$ can be quantified using the distance defined in Section 3.2.

Theorem 4.1. *Let E be the true expectation of a continuous function $u(\xi, y)$ (over $y \in Y$) conditioned on variable $\xi \in Z$, which is associated with a BBA m_ξ with continuous focal elements D_ks. Let $E_n(\xi)$ be its approximation defined as in Eq. (18). Denote the BBA of $E(\xi)$ as m_E with focal elements C_ks, and the BBA of $E_n(\xi)$ be m_{E_n} with focal elements B_ks obtained by the procedure described above. With $\|u(y, \xi) - u_n(y, \xi)\|_{L^p_\eta(Y)} \leq \epsilon_n$ for all $\xi \in Z$ and the assumption that u is continuous over Z, we have*

$$|D_H(m_E, m_{E_n})| \leq \epsilon_n. \tag{23}$$

Proof. From $\|u(y, \xi) - u_n(y, \xi)\|_{L^p_\eta(Y)} \leq \epsilon_n$ for all $\xi \in Z$, one can easily show that for any $\xi \in Z$, the error in the approximation E_n is bounded by the error in the approximation u_n, i.e., we have $|E(\xi) - E_n(\xi)| \leq \epsilon_n$ for any $\xi \in Z$.

Since u and u_n is continuous over Z, their statistics in stochastic space $E(\xi)$ and $E_n(\xi)$ are continuous over Z as well. In addition, all the focal elements of ξ are continuous domains.

Let $D_H(m_E, m_{E_n}) = \sum m_\xi(D_k)d_H(C_k, B_k)$, Using Theorem 3.1, one can easily conclude that the Eq. (23) holds. □

4.3. Algorithm

The steps for obtaining output BBA for $E_n(\xi)$ is outlined in Algorithm 1. The calculation for standard deviation can be performed following the algorithm by replacing $E_n(\xi)$ with $S_n(\xi)$. As describe in Section 2 Problem Setup, the algorithm assumes that PDF is available for random variable y, BBAs are available for each uncertain variable ξ_i. Then we obtain BBA for the full-dimensional variable ξ with hypercubes as focal elements. In each focal element (hypercube), one pairs of optimization are solved to obtain the upper/lower bounds of the focal element interval for the output statistics $E_n(\xi)$. For any fixed ξ, $E_n(\xi)$ is efficiently obtained using gPC expansion over stochastic space Y. Sampling method has been used to solve the optimization problems in our examples, however, it is possible to improve the efficiency of the optimization using multi-start implementations of local optimization methods or efficient global optimization method. Once the output focal elements are obtained, the belief mass can be assigned. With the obtained BBA, CBF and CPF can then be calculated without much computational effort. Since the algorithm goes through all hypercubes, its complexity increases as dimensions of Z or the focal elements of each ξ_i increases. For example, in one-dimensional case, the computational cost increases linearly with the increase in the number of focal elements. With the number of focal elements for each ξ_i fixed, the computational cost will increase exponentially with the increase in the dimension of space Z. As shown in Section 5.2.2, one may also construct computationally cheaper surrogate to approximate the function $E_n(\xi)$ in the space Z to reduce the computational cost, however, with sacrifice on the accuracy of output BBA approximation.

Algorithm 1: Summarized steps for obtaining BBA for $E_n(\xi)$

Input
PDF for $y \in Y$, BBA (focal element D_{i,k_i} with $m_{\xi_i}(D_{i,k_i})$) for each $\xi_i \in Z_i$.

Obtain hypercube focal element D_k and mass for $\xi \in Z$
for all combinations of focal elements from each ξ_i **do**
  Obtain n_Z-dimensional hypercube $D_k = D_{1k_1} \times D_{2k_2} \times \ldots \times D_{n_Z k_{n_Z}}$.
  Assign the mass $m_\xi(D_k) = \Pi_{i=1}^{n_Z} m_{\xi_i}(D_{ik_i})$.
end for

Obtain output focal element and mass
for all focal elements D_k **do**
  Solve optimizations (21)–(22) for $[B_{k,1}, B_{k,2}]$ (call approximation $E_n(\xi)$).
  Assign mass $m([B_{k,1}, B_{k,2}]) = m_\xi(D_k)$.
end for
Obtain CBF and CPF using Eqs. (6)–(7).

Approximation $E_n(\xi)$ (with fixed ξ) using gPC
Specify a set of quadrature points $\{y^j, \alpha^j\}_{j=1}^M$.
Solve system Eq. (1) at quadrature points to obtain $u(y^j, \xi)$.
Perform gPC expansion with Eqs. (14)–(16), obtain $u_n(y, \xi)$.
Obtain $E_n(\xi)$ using Eq. (20).

5. Numerical examples

5.1. Ordinary differential equation (with 1D BBA structure)

We first consider a simple example of an ordinary differential equation (ODE) as

$$\frac{du(t, \xi_1)}{dt} = \xi_1 u, \qquad u(0) = \xi_2, \tag{24}$$

where ξ_1 is a random variable with normal distribution $\mathcal{N}(0, 1)$, and ξ_2 is a non-probabilistic uncertain variable associated with a BBA (the m-function) as

$$m_{\xi_2}(D_1) = 0.2; m_{\xi_2}(D_2) = 0.5; m_{\xi_2}(D_3) = 0.3,$$

where the focal elements D_is are overlapped intervals

$$D_1 = [0.03, 0.045); D_2 = [0.04, 0.055); D_3 = [0.05, 0.06].$$

The goal is to quantify the mixed types of uncertainty in the output solution u propagated from the uncertainty in inputs using the presented numerical method, i.e., representing the aleatory uncertainty using the gPC method and obtain a BBA to quantify the epistemic uncertainty in the conditional expected value of the output u.

Due to the simplicity of the chosen ODE Eq. (24), not only the analytical solution for the output is known $u(t, \xi_1, \xi_2) = \xi_2 e^{\xi_1 t}$, but also the analytical solution for the conditional expectation of the output is available $E(u|\xi_2, t) = \xi_2 e^{t^2/2}$. The

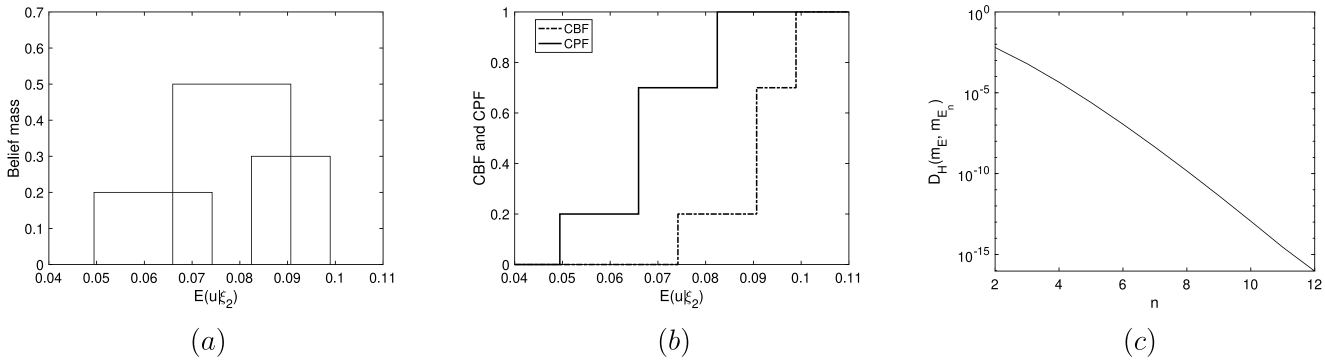

Fig. 1. (a) The BBA for numerical conditional expectation with approximation order $n = 6$, (b) The CBF and CPF for $E(u|\xi_2)$, and (c) The distance $D_H(m_E, m_{E_n})$ with respect to approximation order n.

analytical solutions can be used for error analysis of the numerical approach. In this problem, we consider the solution u at a fixed time $t = 1$.

To quantify the aleatory uncertainty in the system efficiently, we implement the gPC expansion with polynomial order n to obtain $u_n(\xi_1, \xi_2) = \sum_{j=0}^{n} u_j(\xi_2)\Phi_j(\xi_1)$, which serves as an approximation to the exact solution u. Then the approximation of conditional expectation E_n (depending on ξ_2) is consequently calculated from u_n. Following that, the BBA of numerical conditional expectation m_{E_n} is then constructed. The focal elements of the obtained BBA (see Fig. 1(a)) with approximation order $n = 6$ are

$$B_1 = [0.0495, 0.0742], \qquad B_2 = [0.0659, 0.0907], \qquad B_3 = [0.08240.0990];$$

and the assigned masses are

$$m_{E_n}([B_1]) = 0.2, \qquad m_{E_n}([B_2]) = 0.5, \qquad m_{E_n}([B_3]) = 0.3. \tag{25}$$

From the BBA, one can conclude that the expectation of the output solution will be inside the interval [0.0659, 0.0907] with maximum degree of belief 0.5, and no preference will be given to any more specific subset of that interval due to the epistemic uncertainty. With obtained BBA m_{E_n}, the cumulative belief function (CBF) is calculated as follows:

$$CBF(z) = Bel(\{\xi|\xi \le z\}) = \sum_i m_{E_n}(B_i|B_i \subseteq \{\xi|\xi \le z\})$$
$$= \begin{cases} 0, & \text{for } z < 0.0742, \\ m_{E_n}([B_1]) = 0.2, & \text{for } 0.0742 \le z < 0.0907, \\ m_{E_n}([B_1]) + m_{E_n}([B_2]) = 0.7, & \text{for } 0.0907 \le z < 0.0990, \\ m_{E_n}([B_1]) + m_{E_n}([B_2]) + m_{E_n}([B_3]) = 1, & \text{for } z \ge 0.0990. \end{cases} \tag{26}$$

The cumulative plausibility function (CPF) is calculated as follows:

$$CPF(z) = Pl(\{\xi|\xi \le z\}) = \sum_i m_{E_n}(B_i|B_i \cap \{\xi|\xi \le z\} \ne \emptyset)$$
$$= \begin{cases} 0, & \text{for } z < 0.0495, \\ m_{E_n}([B_1]) = 0.2, & \text{for } 0.0495 \le z < 0.0659, \\ m_{E_n}([B_1]) + m_{E_n}([B_2]) = 0.7, & \text{for } 0.0659 \le z < 0.0824, \\ m_{E_n}([B_1]) + m_{E_n}([B_2]) + m_{E_n}([B_3]) = 1, & \text{for } z \ge 0.0824. \end{cases} \tag{27}$$

The CBF and CPF are plotted in Fig. 1(b), which bound the possible true cumulative distribution function (CDF) of the expectation of output $E(u|\xi_2)$. We also study the convergence of the distance between the true BBA and the one based on approximation with respect to polynomial order n. The error in the BBA obtained based on numerical approximation m_{E_n} is plotted in Fig. 1(c) with respect to the approximation order n. Clearly one can observe the spectral convergence.

Similarly, the BBA of numerical conditional standard deviation m_{S_n} is also constructed. The obtained BBA, CBF/CPF with approximation order $n = 6$ are provided in Fig. 2(a,b). The output BBA shows that the standard deviation will be inside the interval [0.0863, 0.1187] with maximum degree of belief 0.5, and no preference will be given to any more specific subset of that interval due to the epistemic uncertainty. The analytical solution for the conditional standard deviation of the output is also available and the formula is $S(u|\xi_2, t = 1) = \xi_2\sqrt{e^2 - e}$. The analytical solutions is also used to study the convergence of the distance between the true BBA and the one based on approximation with respect to polynomial order n. The error in the BBA m_{S_n} is plotted in Fig. 2(c). Clearly one can again observe the spectral convergence with respect to polynomial order n.

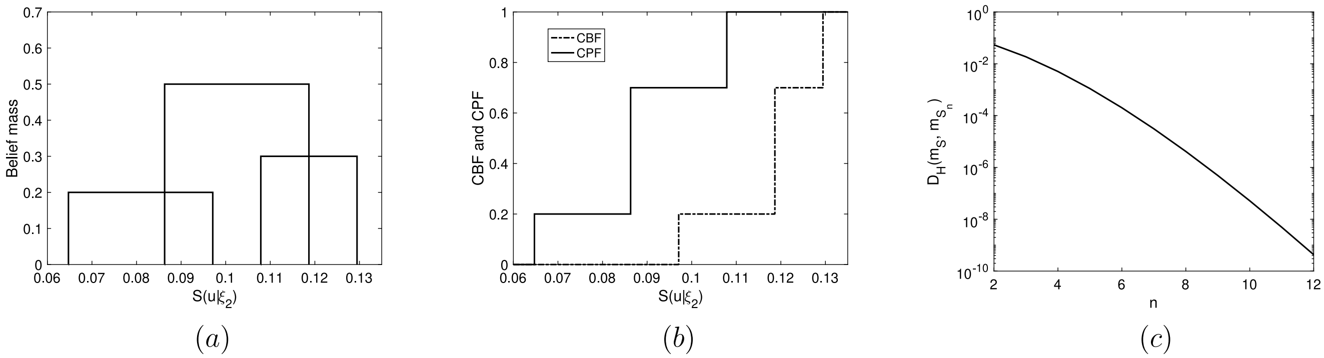

Fig. 2. (a) The BBA for numerical conditional standard deviation with approximation order $n = 6$, (b) The CBF and CPF for $S(u|\xi_2)$, and (c) The distance $D_H(m_S, m_{S_n})$ with respect to approximation order n.

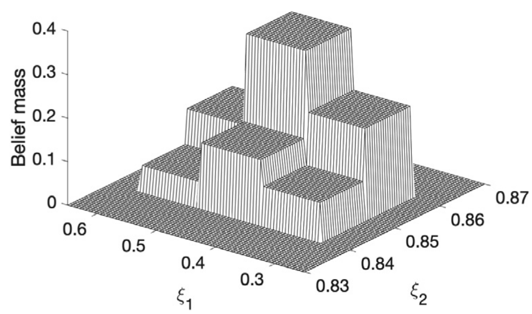

Fig. 3. 2D belief structure of the BBA for input.

5.2. Nonlinear ordinary differential equation (with 2D BBA structure)

5.2.1. Mixed uncertainty quantification

We now consider a nonlinear ODE equation.

$$\frac{du(t,y,\xi_1)}{dt} = -\xi_1 u(1-\frac{u}{y}), \qquad u(0) = \xi_2, \tag{28}$$

where we consider y to be random variable uniformly distributed over interval $[1, 3]$, and ξ_1, ξ_2 to be uncertain with BBAs as

$$m_{\xi_1}([0.3, 0.4]) = 0.3;\ m_{\xi_1}([0.4, 0.5]) = 0.5;\ m_{\xi_1}([0.5, 0.6]) = 0.2,$$
$$m_{\xi_2}([0.84, 0.85]) = 0.3;\ m_{\xi_2}([0.85, 0.86]) = 0.7.$$

The 2D belief structure of the BBA is shown in Fig. 3.

The analytical solutions are available for error analysis. The solution to ODE is

$$u(t,y,\xi_1,\xi_2) = \frac{y\xi_2 e^{-\xi_1 t}}{\xi_2 e^{-\xi_1 t} - \xi_2 + y}, \tag{29}$$

and the solution for the conditional expectation of the output is

$$E(u|\xi_1,\xi_2,t) = \xi_2 e^{-\xi_1 t} - \frac{\xi_2 e^{-\xi_1 t}(\xi_2 e^{-\xi_1 t} - \xi_2)}{2} log\left|\frac{3+\xi_2 e^{-\xi_1 t} - \xi_2}{1+\xi_2 e^{-\xi_1 t} - \xi_2}\right|.$$

and the solution for the conditional standard deviation of the output is

$$S^2(u|\xi_1,\xi_2,t) = \xi_2^2 e^{-2\xi_1 t} - \xi_2^2 e^{-2\xi_1 t}(\xi_2 e^{-\xi_1 t} - \xi_2) log\left|\frac{3+\xi_2 e^{-\xi_1 t} - \xi_2}{1+\xi_2 e^{-\xi_1 t} - \xi_2}\right|$$
$$+\frac{1}{2}\xi_2^2 e^{-2\xi_1 t}(\xi_2 e^{-\xi_1 t} - \xi_2)^2 (1 + \frac{1}{\xi_2 e^{-\xi_1 t} - \xi_2 + 1} + \frac{1}{\xi_2 e^{-\xi_1 t} - \xi_2 + 3}).$$

Here, we consider u at a fixed time $t = 2$, and construct the gPC expansion (over stochastic space $y \in [1, 3]$) u_n (n is the highest polynomial order) to approximate the exact solution u. Consequently, the approximation of conditional expectation E_n (depending on ξ_1, ξ_2), and associated BBA can be calculated/constructed from u_n. The obtained BBA with

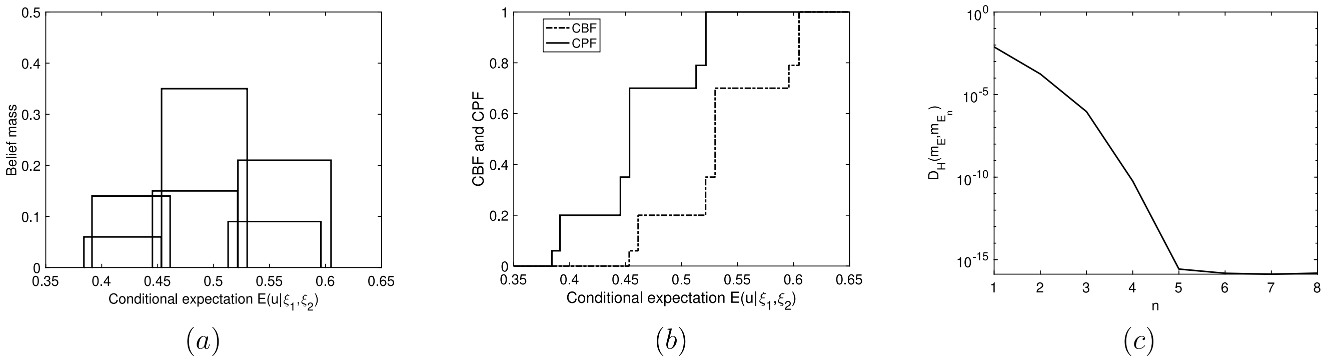

Fig. 4. (a) The BBA for numerical conditional expectation with approximation order $n = 4$, (b) The CBF and CPF for $E(u|\xi_1, \xi_2)$, and (c) The distance $D_H(m_E, m_{E_n})$ with respect to approximation order n.

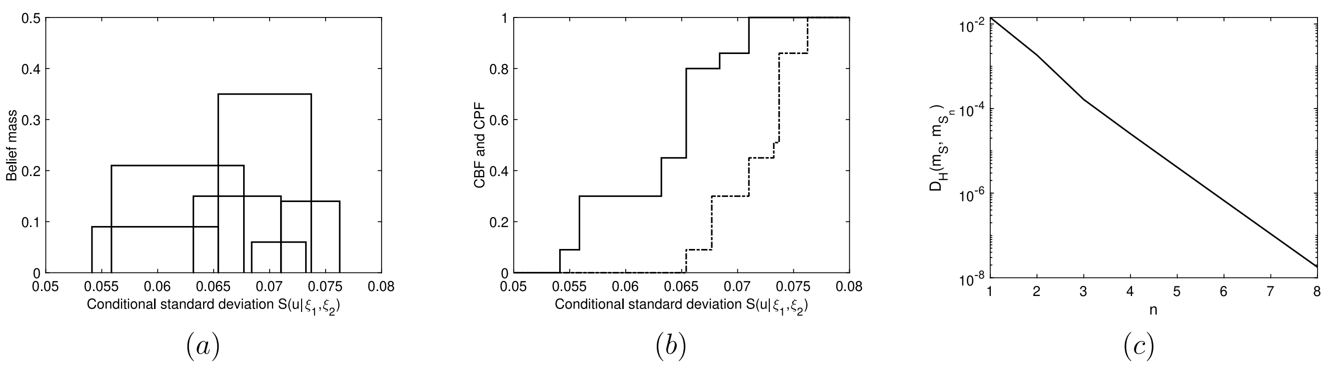

Fig. 5. (a) The BBA for numerical conditional standard deviation with approximation order $n = 4$, (b) The CBF and CPF for $S(u|\xi_1, \xi_2)$, and (c) The distance $D_H(m_S, m_{S_n})$ with respect to approximation order n.

approximation order $n = 4$ is provided in Fig. 4(a), which shows that the expectation of the output solution will be inside the interval [0.453, 0.53] with maximum degree of belief 0.35. Similarly, the CBF and CPF are constructed and plotted in Fig. 4(b). We also study the convergence of the distance between the true BBA and the one based on approximation with respect to polynomial order n for this nonlinear problem. Fig. 4(c) shows the spectral convergence of the numerical approach with respect to order n.

Similarly, the approximation of conditional standard deviation $S_n(\xi_1, \xi_2)$, and associated BBA, CBF/CPF can be calculated/constructed from u_n (see Fig. 5(a,b)). The output BBA with $n = 4$ shows that the standard deviation of the output solution will be inside the interval [0.0654, 0.0737] with maximum degree of belief 0.35. The distance between the true BBA and the one based on approximation with respect to polynomial order n for standard deviation is also calculated and plotted in Fig. 5(c), which shows the spectral convergence of the numerical approach with respect to order n.

5.2.2. Comparison to approach with surrogate over non-probabilistic space

Recall that our proposed approach constructs gPC expansion as an approximation only in the probabilistic space Y, not in the non-probabilistic space Z. To further reduce the computational cost, surrogate has been used in non-probabilistic space Z to estimate the lower and upper bounds of output focal elements as in [43]. For the purpose of demonstration, we also construct surrogate of gPC expansion to approximate $E_4(\xi)$ and $S_4(\xi)$ in the non-probabilistic space $\xi \in Z$ for this simple example, and compare the obtained CBF/CPF to the ones produced by our approach. Fig. 6(a) shows the comparison of CBF/CPF of $E(u|\xi_1, \xi_2)$, the curves in black color from our approach are exactly overlapped with the truth (therefore truth is not plotted for better visualization), while the curves from the approach with surrogate constructed in non-probabilistic space Z are almost overlapping (with almost invisible but slight deviation around $E = 0.605$). The comparison of CBF/CPF for $S(u|\xi_1, \xi_2)$ are shown in Fig. 6(b,c), from which one can observe that CBF/CPF from our approach is closer to (almost overlapping with) the truth. The observations match the expectation that our method would produce more accurate result since no approximation is used in space Z from our proposed approach.

To further compare the two approaches, the errors in the obtained BBAs are calculated for both expectation and standard deviation from both methods. From Table 1, one can also conclude that our method produce more accurate BBAs for both expectation and standard deviation.

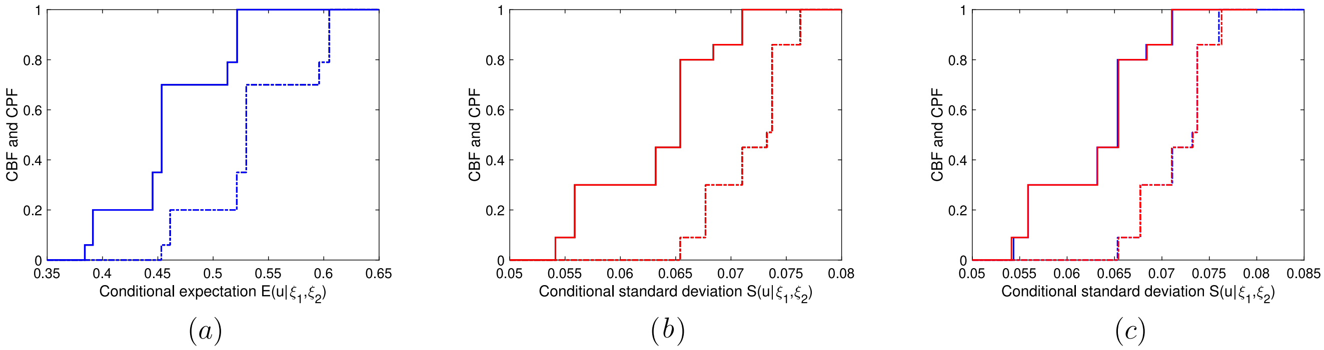

Fig. 6. CBF and CPF: (a) comparison on the expectation $E(u|\xi_1, \xi_2)$ between our approach (black) and the approach with surrogate in non-probabilistic space Z (blue); (b) comparison on the standard deviation $S(u|\xi_1, \xi_2)$ from our approach (black) to the truth (red); and (c) comparison on the standard deviation $S(u|\xi_1, \xi_2)$ from the approach with surrogate in non-probabilistic space Z (blue) to the truth (red).

Table 1
Error in BBAs of expectation and standard deviation.

	Our method	Method with surrogate constructed over Z
Error in BBA of $E(u\|\xi_1, \xi_2)$	5.76e−11	1.18e−04
Error in BBA of $S(u\|\xi_1, \xi_2)$	2.53e−05	8.9e−05

5.3. Quasi-one-dimensional nozzle flow

The quasi-one-dimensional (Q1D) nozzle problem is a simple example of aerodynamic flows. In a quasi-one-dimensional (convergent–divergent) nozzle shocked flow, the impact of the uncertain inlet conditions, exit pressure and nozzle geometry on the output has been analyzed. For example, Mathelin and Hussaini [3] analyzed the uncertainty in the exit pressure and exit velocity of supersonic flow using a stochastic collocation method. In their work, it was assumed that only aleatory uncertainty exists in the input parameters and nozzle geometry. Chen et al. [44] quantified the uncertainty of the shock position in a dual throat nozzle with a simplified model. Different probability density functions were assigned to the initial velocity and the corresponding PDFs for the shock position were obtained using the PC expansion. Abgrall et al. [45] introduced a semi-intrusive method to analyze the uncertainty in Mach number within the Q1D nozzle flow with random heat coefficient ratio. They compared the convergence rates for the standard deviation of Mach number between the semi-intrusive method and gPC expansion. The works mentioned above mainly focused on aleatory uncertainty where PDFs were prescribed for random input variables, however, the PDFs might not always be available and epistemic uncertainty may be involved. Therefore it is crucial to explore mixed types of uncertainty in Q1D flow. Roy and Oberkampf [19] were interested in the total predictive uncertainty in the test section temperature in the Q1D flow. Interval analysis coupled with the Monte Carlo method was implemented to obtain a "p-box" to represent the propagated uncertainty in the temperature from the input parameters, followed by appending the numerical and the model uncertainty into the p-box. However, it could be computationally expensive due to the slow convergence of the Monte Carlo method. In this section, we apply the presented numerical procedure that couples gPC expansion method and DS theory to quantify the mixed types of uncertainty in the shock position of Q1D flow.

5.3.1. Basic equations

The system of Euler equations of the conservative form governing the Q1D nozzle flow can be described as follows:

$$U_t + F(U)_x = S(U) \tag{30}$$

where

$$U = \begin{Bmatrix} \rho A \\ \rho u A \\ \rho \mathbf{E} A \end{Bmatrix}, F = \begin{Bmatrix} \rho u A \\ (\rho u^2 + p)A \\ (\rho \mathbf{E} + p)uA \end{Bmatrix}, S = \begin{Bmatrix} 0 \\ pA_x \\ -pA_t \end{Bmatrix},$$

with ρ as the density, u as the velocity, A as the cross-section area, p as the pressure and $\mathbf{E}$ as the total energy. In the formulation, $\rho\mathbf{E} = \frac{p}{\gamma-1} + \frac{1}{2}\rho u^2$, $A_x = \frac{\partial(A)}{\partial x}$ and $A_t = \frac{\partial(A)}{\partial t}$.

The shock position x_s of the flow in the steady case is the quantity of our interest. With the isentropic flow relation before/after the occurrence of the shock and the Rankine–Hugoniot relation at the shock position, an implicit function for x_s dependent on only A and $\frac{p_2}{p_1}$ can be derived, where p_1, p_2 are inlet and exit pressures, respectively. Therefore, the cross section area A, inlet and exit pressures are considered as uncertain in the current work. The inlet temperature $T = 0.7469$ is considered as a deterministic parameter hereafter.

5.3.2. Mathematical representation of mixed uncertainty

The nozzle geometry has an inevitable level of variability due to manufacturing limitations. Therefore, we assume that cross-section area $A(x)$ varies with space with mean value defined as

$$\bar{A}(x) = \begin{cases} 0.7, & x <= 0.25 \\ 25.6x^3 - 28.8x^2 + 9.6x - 0.3, & 0.25 < x <= 0.5 \\ -1.6x^3 + 4.0x^2 - 2.8x + 1.1, & 0.5 < x <= 1 \end{cases}$$

A Gaussian process is further assumed for nozzle geometry and its correlation along the x direction is:

$$C_{AA}(x_1, x_2) = \sigma^2 e^{-\frac{|x_1 - x_2|}{b}}, \quad (31)$$

where $b = 10$ is the correlation length and $\sigma = 0.01$ is the associated standard deviation. For the purpose of numerical computation, we represent the stochastic field using the Karhunen–Loeve decomposition,

$$A(x) = \bar{A}(x) + \sum_{i=1}^{\infty} \sqrt{\lambda_i} \Psi_i(x) \xi_i, \quad (32)$$

where ξ_is are independent standard Gaussian variables and λ_i, Ψ_i are eigenvalue, eigenfunctions of the correlation function satisfying

$$\int C_{AA}(x_1, x_2) \Psi_i(x_2) dx_2 = \lambda_i \Psi_i(x_1) \text{ on } [0, 1]. \quad (33)$$

Due to the rapid decay of eigenvalues λ_i as i increases, the terms with $i \geq 3$ in the expansion are truncated. Then the nozzle geometry is described as

$$A(x) = \bar{A}(x) + \sqrt{\lambda_1} \Psi_1(x) \xi_1 + \sqrt{\lambda_2} \Psi_2(x) \xi_2, \qquad \xi_1 \sim \mathcal{N}(0, 1), \xi_2 \sim \mathcal{N}(0, 1). \quad (34)$$

The exit pressure p_2 is also assumed to be stochastic and characterized by a Gaussian variable

$$p_2 = 0.86 * 0.6171 + 0.01\xi_3, \qquad \xi_3 \sim \mathcal{N}(0, 1). \quad (35)$$

The inlet pressure p_1 is assumed to be non-probabilistic and characterized by the following BBA with universal set $X_{p_1} = [0.59, 0.65]$:

$$m_{p_1}(D_1) = 0.1573, m_{p_1}(D_2) = 0.6827, m_{p_1}(D_3) = 0.1573, m_{p_1}(D_4) = 0.0027,$$

where the focal elements D_is are

$$D_1 = [0.59, 0.61); D_2 = [0.61, 0.63); D_3 = [0.63, 0.65]; D_4 = X_{p_1}.$$

5.3.3. Results

The presented method is implemented to quantify the aleatory and epistemic uncertainty in the shock position x_s. First, the shock position is expanded in the probability space in terms of Hermite polynomials:

$$x_s(\xi_1, \xi_2, \xi_3, p_1) = \sum_{i=0}^{N} x_{si}(p_1) \Phi_i(\xi_1, \xi_2, \xi_3). \quad (36)$$

Then consider the conditional expectation of shock position $E[x_s|p_1] = \bar{x}_s(p_1)$. Since p_1 is uncertain and represented by a BBA, consequently, the output $\bar{x}_s$ is also nondeterministic and its BBA can be obtained using the method in Section 4.2. From the BBA of $E[x_s|p_1]$ shown in Fig. 7(a), we conclude that (1) the expectation of the shock position falls inside $H = [0.816, 0.853]$ with the highest degree of belief $Bel(E[x_s|p_1] \in H) = 0.6827$ and (2) no further preference inside the interval $H = [0.816, 0.853]$. Fig. 7(b) shows the CBF and CPF, which bound the possible true CDF of the expectation of the shock position. For example, consider the proposition "$E[x_s|p_1] < 0.83$" and estimate the likelihood of its occurrence. From Fig. 7(b), we conclude that the lower and upper bounds of the probability of this proposition being true are:

$$Bel(E[x_s|p_1] < 0.83) \leq \mathbf{P}(E[x_s|p_1] < 0.83) \leq Pl(E[x_s|p_1] < 0.83),$$

where belief and plausibility are calculated based on the obtained belief function in Fig. 7(a).

$$\begin{aligned} Bel(E[x_s|p_1] < 0.83) &= m([0.775, 0.816]) = 0.1573, \\ Pl(E[x_s|p_1] < 0.83) &= m([0.775, 0.816]) + m([0.816, 0.853]) + m([0.775, 0.888]) = 0.8427. \end{aligned}$$

The conditional standard deviation of shock position $S[x_s|p_1]$ is also considered, and its BBA and CBF, CPF are provided in Fig. 8. One can easily observe that the standard deviation of shock position falls inside the interval [0.02157, 0.02234] with the highest degree of belief 0.6827. If consider the proposition "$S[x_s|p_1] < 0.022$", the likelihood of its occurrence would be bounded by the belief of the proposition 0.1537 and the plausibility of the proposition 0.8427 (read from the curves of Fig. 8(b)).

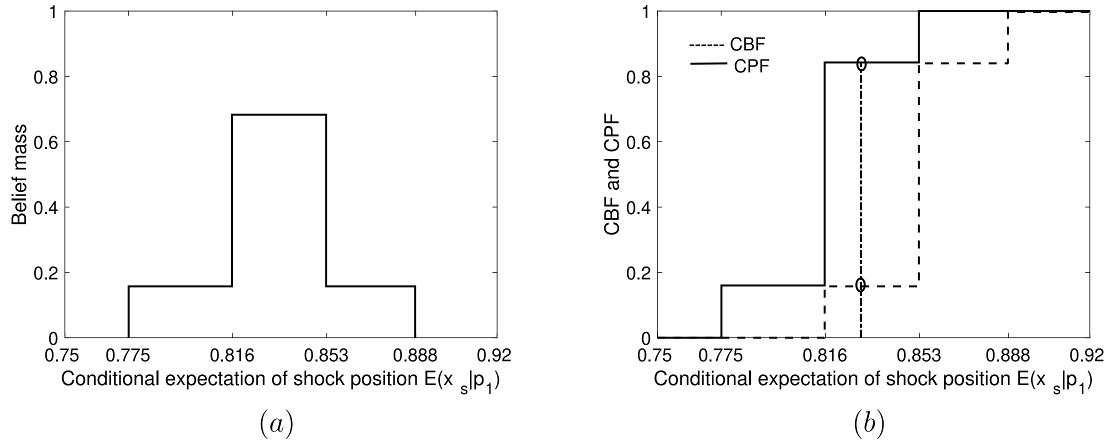

Fig. 7. (a) The belief function of the conditional expectation $E[x_s|p_1]$. (b) The CBF/CPF of the conditional expectation $E[x_s|p_1]$.

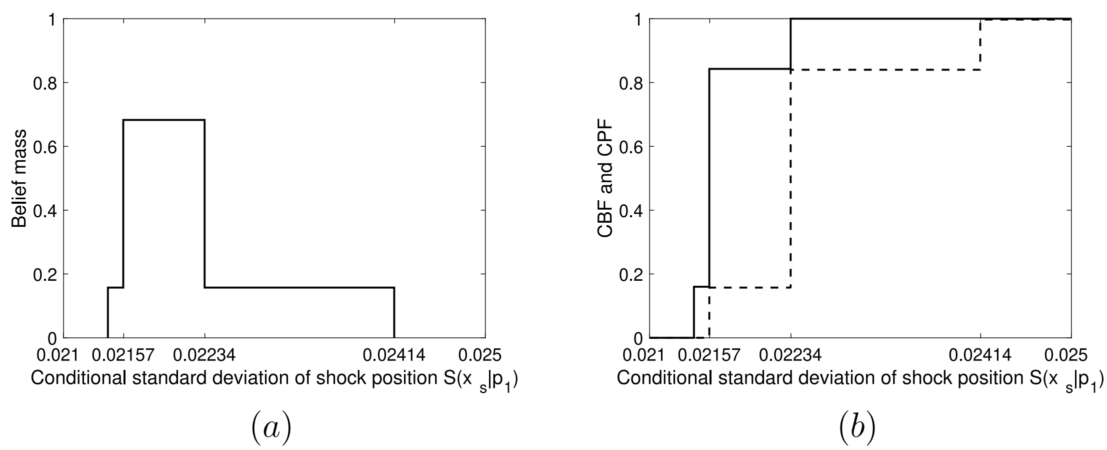

Fig. 8. (a) The belief function of the conditional standard deviation $S[x_s|p_1]$. (b) The CBF/CPF of the conditional standard deviation $S[x_s|p_1]$.

6. Summary and conclusions

In this work, we introduce the relevant theoretical basics from DS theory, present the numerical approach based on DS theory combined with gPC expansion for mixed types of uncertainty propagation, and conduct the error analysis. Specifically, we use definition of the extension principle for random sets directly in the framework of DS theory due to the equivalence between the BBA and random sets. The extension principle uniquely defines the BBA for model output mapped (through a function) from inputs characterized with BBAs. Then we present the numerical approach for mixed types of uncertainty propagation in the system where gPC method is used for efficiently propagating aleatory uncertainty represented using PDFs and the extension principle is used for propagating epistemic uncertainty represented with BBAs. The approach first estimates the statistics of the output solution in the stochastic space, and then represents the epistemic uncertainty in the statistics using a BBA. In order to analyze the error in the obtained BBA based on the numerical approximation, a measure based on Hausdorff distance is defined to quantify the difference between two BBAs. Using simple ODE examples with available analytical statistics, it is demonstrated that exponentially-fast convergence rate can be obtained for the numerical estimations of the output solutions involving propagated mixed types of uncertainty.

Data availability

No data was used for the research described in the article.

Acknowledgments

This work was supported by National Science Foundation, United States (DMS-2152040).

References

[1] N. Wiener, The homogeneous chaos, Amer. J. Math. 60 (4) (1938) 897–936.
[2] D. Xiu, G. Karniadakis, The Wiener-askey polynomial chaos for stochastic differential equations, SIAM J. Sci. Comput. 24 (2) (2002) 619–644.
[3] L. Mathelin, M.Y. Hussaini, A Stochastic Collocation Algorithm for Uncertainty Analysis, Tech. Rep. NASA/CR-2003-212153, NASA Langley Research Center, 2003.
[4] Y. He, M. Razi, C. Forestiere, L.D. Negro, R.M. Kirby, Uncertainty quantification guided robust design for nanoparticles' morphology, Comput. Methods Appl. Mech. Engrg. 336 (2018) 578–593.
[5] R. Schobi, B. Sudret, J. Wiart, Polynomial-chaos-based kriging, Int. J. Uncertain. Quantif. 5 (2015) 171–193.
[6] W.L. Oberkampf, J.C. Helton, K. Sentz, Mathematical representation of uncertainty, in: Proceedings of the AIAA Non-Deterministic Approaches Forum AIAA 2001-1645, 2001.
[7] L.A. Zadeh, Fuzzy sets, Inf. Control 8 (1965) 338–353.
[8] P. Walley, G.D. Cooman, A behavioural model for linguistic uncertainty, Inform. Sci. 134 (2001) 1–37.
[9] D. Dubois, H. Prade, Possibility Theory: an Approach to Computerized Processing of Uncertainty, Plenum Press, New York, 1988.
[10] D. Didier, Possibility theory and statistical reasoning, Comput. Statist. Data Anal. 51 (1) (2006) 47–69.
[11] S. Destercke, D. Dubois, E. Chojnachi, Unifying practical uncertainty representations: I. generalized p-boxes, Internat. J. Approx. Reason. 49 (2008) 649–663.
[12] G. Shafer, A Mathematical Theory of Evidence, Princeton University Press, N.J.,US, 1976.
[13] A.P. Dempster, Upper and lower probabilities induced by a multi-valued mapping, Ann. Math. Statist. 38 (1967) 325–339.
[14] J. Jakeman, M. Eldred, D. Xiu, Numerical approach for quantification of epistemic uncertainty, J. Comput. Phys. 229 (2010) 4648–4663.
[15] X. Chen, Y. He, D. Xiu, An efficient method for uncertainty propagation using fuzzy sets, SIAM J. Sci. Comput. 37 (6) (2015) 2488–2507.
[16] Y. He, M. Mirzargar, R.M. Kirby, Mixed aleatory and epistemic uncertainty quantification using fuzzy set theory, Internat. J. Approx. Reason. 66 (2015) 1–15.
[17] C. Wang, Z. Qiu, Y. He, Fuzzy interval perturbation method for the uncertain heat conduction problem with interval and fuzzy parameters, Internat. J. Numer. Methods Engrg. 104 (2015) 330–346.
[18] C. Baudrit, D. Dubois, D. Guyonnet, Joint propagation and exploitation of probabilistic and possibilistic information in risk assessment, IEEE Trans. Fuzzy Syst. 14 (5) (2006) 593–608.
[19] C.J. Roy, W.L. Oberkampf, A comprehensive framework for verification, validation, and uncertainty quantification in scientific computing, Comput. Methods Appl. Mech. Engrg. 200 (2011) 2131–2144.
[20] B. Lockwood, M. Anitescu, F. Mavripilis, Mixed aleatory/epistemic uncertainty quantification for hypersonic flows via gradient-based optimization and surrogate models, in: Proceedings of the 50th AIAA Aerospace Sciences Meeting, AIAA2012-1254 Nashville, TN, 2012.
[21] C. Wang, Z. Qiu, M. Xu, Y. Li, Novel reliability-based optimization method for thermal structure with hybrid random, interval and fuzzy parameters, Appl. Math. Model. 47 (2017) 573–586.
[22] A. Talavera, R. Aguasca, B. Galván, A. Cacereño, Application of demster-Shafer theory for the quantification and propagation of the uncertainty caused by the use of AIS data, Reliab. Eng. Syst. Saf. 111 (2013) 95–105.
[23] J. Tang, Z. Wu, C. Yang, Epistemic uncertainty quantification in flutter analysis using evidence theory, Chin. J. Aeronaut. 28 (2015) 897–936.
[24] N.B. Abdallah, N. Mouhous-Voyneau, T. Denoeux, Using Dempster-Shafer theory to model uncertainty in climate change and environmental impact assessments, in: Proceedings of the 16th International Conference on Information Fusion, Istanbul, Turkey, 2013, pp. 2117–2124.
[25] H.R. Bae, R.V. Grandhi, R.A. Canfield, Uncertainty quantification of structural response using evidence theory, AIAA J. 41 (10) (2003) 2062–2068.
[26] C. Wang, H.G. Matthies, Epistemic uncertainty-based reliability analysis for engineering system with hybrid evidence and fuzzy variables, Comput. Methods Appl. Mech. Engrg. 355 (2019) 438–455.
[27] H. Shah, S. Hosder, T. Winter, A mixed uncertainty quantification approach using evidence theory and stochastic expansions, Int. J. Uncertain. Quantif. 5 (1) (2015) 21–48.
[28] G. Tang, L.P. Swiler, M.S. Eldred, G. Iaccarino, Using stochastic expansion methods in evidence theory for mixed aleatory-epistemic uncertainty quantification, in: Proceeding of the 12th AIAA Non-Deterministic Approaches Conference, Orlando, FL, 2010.
[29] M.S. Eldred, L.P. Swiler, G. Tang, Mixed aleatory-epistemic uncertainty quantification with stochastic expansions and optimization-based interval estimation, Reliab. Eng. Syst. Saf. 96 (2011) 1092–1113.
[30] D. Dubois, H. Prade, Random sets and fuzzy interval analysis, Fuzzy Sets and Systems 42 (1991) 87–101.
[31] T. Denaeux, Extending stochastic ordering to belief functions on the real line, Inform. Sci. 179 (2009) 1362–1376.
[32] A.L. Jousselme, P. Maupin, Distances in evidence theory: Comprehensive survey and generalizations, Internat. J. Approx. Reason. 53 (2012) 118–145.
[33] M. Loudahi, J. Klein, J. Vannobel, O. Colot, New distances between bodies of evidence based on Dempsterian specialization matrices and their consistency with the conjunctive combination rule, Internat. J. Approx. Reason. 55 (5) (2014) 1093–1112.
[34] M.C. Florea, A. Jousselme, É. Bosseé, D. Grenier, Robust combination rules for evidence theory, Inf. Fusion 10 (2009) 183–197.
[35] F. Tonon, A. Bernardini, A. Mammino, Reliability analysis of rock mass response by means of random set theory, Reliab. Eng. Syst. Saf. 42 (1991) 263–282.
[36] I.R. Goodman, H.T. Nguyen, Uncertainty Models for Knowledge-Based Systems; a Unified Approach to the Measurement of Uncertainty, Elsevier Science Inc., New York, NY, USA, 1985.
[37] H.T. Nguyen, On random sets and belief functions, J. Math. Anal. Appl. 65 (1978) 531–542.
[38] R.R. Yager, Cumulative distribution functions from Dempster-Shafer belief structures, IEEE Trans. Syst. Man Cybern. 34 (5) (2004) 2080–2087.
[39] R. Cameron, W. Martin, The orthogonal development of nonlinear functionals in series of Fourier–Hermite functionals, Ann. of Math. 48 (2) (1947) 385–392.
[40] R.G. Ghanem, P.D. Spanos, Stochastic Finite Elements: A Spectral Approach, Springer, New York, 1991.
[41] D. Xiu, Numerical Methods for Stochastic Computations: A Spectral Method Approach, Princeton University Press, New Jersey, 2010.
[42] F. Heiss, V. Winschel, Likelihood approximation by numerical integration on sparse grids, J. Econometrics 144 (2008) 62–80.
[43] C. Wang, H. Matthies, Evidence theory-based reliability optimization design using polynomial chaos expansion, Comput. Methods Appl. Mech. Engrg. 341 (2018) 640–657.
[44] L. Chen, W. Shi, Y. Deng, Z. Zhu, A new fusion approach based on distance of evidences, J. Zhejiang Univ. Sci. 6A (5) (2005) 476–482.
[45] R. Abgrall, P.M. Congedoy, C. Correy, S. Galéra, A simple semi-intrusive method for uncertainty quantification of shocked flows, comparison with a non-intrusive polynomial chaos method, in: Proceeding of the Fifth European Conference on Computational Fluid Dynamics, Lisbon, Portugal, 2010.